# Persistent Coverage of a Two-dimensional Manifold Subject to Time-varying Disturbances

William Bentz and Dimitra Panagou

***Abstract*— This paper presents a persistent coverage algorithm for multiple agents subject to 3-D rigid body kinematics. Each agent uses a forward-facing sensing footprint, modeled as an anisotropic spherical sector, to cover a 2-D manifold. The manifold is subject to continual collisions by high speed particles. Particle trajectories are estimated online with an extended Kalman filter using noisy spherical coordinate position measurements. Predicted impact points for each particle, along with associated covariances, are used to generate normally distributed coverage decay. This directs agents to explore in the vicinity of both future and past impact points. The efficacy of the algorithm is demonstrated through simulation.**

## I. Introduction

In the last several years, autonomous research platforms have surged in popularity with the reductions in cost and improved performance of embedded computers. The ubiquity of these systems has spurred great research interest in the development of mobile sensor networks (MSN's). These networks are useful in a variety of applications including: battlefield surveillance [1], search and rescue operations [2], and hull inspections [3], [4]. These underlying control problems of these inspection and surveillance tasks are often referred to in the literature as coverage control.

Coverage is typically classified as either static or dynamic. Static coverage problems (e.g., area coverage, k-coverage and point coverage) often involve driving sensors into an optimal steady state arrangement to survey a domain. This topic has been studied at length in [5]–[7]. Dynamic coverage problems often require the design of control laws that sweep limited range sensing footprints over a domain until all points have been covered up to a satisfactory level in time [8]–[10]. Persistent coverage, the focus of this work, is similar to dynamic coverage; however, the domain is never fully surveyed. Rather, persistent coverage may require continual observation of points for all time.

In [11], a seminal work on persistent coverage, the authors seek to cover all points of a convex polygonal domain in $\mathbb{R}^2$ at least once per time period $T^\star$. This is accomplished by designing concentric closed trajectories for each agent in the network. The authors of [12] maintain similar trajectories and $T^\star$ servicing requirements while introducing a constant coverage decay rate for select points of interest. Speed control along the path yields additional observation time for these points. This is similar to work presented in [13] where the agents travel along closed paths in $\mathbb{R}^2$ sweeping a domain whose coverage level decays linearly in time.

Uniform coverage decay rates over a domain are also considered in [14] and [15]. In these papers, the desired coverage level of the domain is augmented by a density map to yield additional observation time at select areas of interest. In [15] the maps are time-invariant while [14] considers time-varying density maps that may be designed around moving points of interest (e.g., aerial surveillance targets). In these papers, the density maps have no effect upon the coverage decay rate and no methods are proposed for the online estimation of these maps. The presence of a moving target through the domain is essentially forgotten by the agents the moment the target exits the domain. This necessitates that agents must travel faster than targets in order to cover points associated with peaks in the density function before they vanish.

A common thread through the above works is the assumption that all points of interest lie in convex 2-D sets. In [16], the authors design time-optimal trajectories in $\mathbb{R}^3$ that allow for coverage of 2.5 dimensional nonplanar surfaces. However, this work does not consider coverage decay and the agents are once again constrained to preplanned trajectories.

The novel contribution of this paper is a persistent coverage algorithm for non-planar 2-D surfaces embedded in $\mathbb{R}^3$. The algorithm utilizes a time-varying density function, which is estimated online via extended Kalman Filter, to directly encode coverage decay over the surface. This encodes a memory effect which drives agents to inspect areas of the surface that have been or will soon be impacted by moving targets. This paper assumes the 3-D kinematic and sensing models for agents presented in the authors' previous work in [17], [18].

This paper is organized as follows: Section II describes the agent kinematic and sensing models and defines coverage over our surface of interest. In Section III, the coverage control laws and collision avoidance terms are derived. Section IV presents the particle trajectory state estimator and defines our coverage decay rate map. Simulation results and conclusions are presented in Sections V and VI respectively.

## II. Problem Formulation

Consider a network of spherical autonomous agents indexed $i \in \{1, ..., N\}$, of radius $r_i$, whose motion is subject

William Bentz is with the Department of Aerospace Engineering, University of Michigan, Ann Arbor; wbentz@umich.edu.

Dimitra Panagou is with the Department of Aerospace Engineering, University of Michigan, Ann Arbor; dpanagou@umich.edu.

The authors would like to acknowledge the support of the Automotive Research Center (ARC) in accordance with Cooperative Agreement W56HZV-14-2-0001 U.S. Army TARDEC in Warren, MI and the support by an Early Career Faculty grant from NASAs Space Technology Research Grants Program

to 3-D rigid body kinematics [19]:

$$\begin{bmatrix}\dot{x}_i\\ \dot{y}_i\\ \dot{z}_i\end{bmatrix} = \begin{bmatrix}\cos\Theta_i\cos\Psi_i & \sin\Phi_i\sin\Theta_i\cos\Psi_i - \cos\Phi_i\sin\Psi_i & \cos\Phi_i\sin\Theta_i\cos\Psi_i + \sin\Phi_i\sin\Psi_i\\ \cos\Theta_i\sin\Psi_i & \sin\Phi_i\sin\Theta_i\sin\Psi_i + \cos\Phi_i\cos\Psi_i & \cos\Phi_i\sin\Theta_i\sin\Psi_i - \sin\Phi_i\cos\Psi_i\\ -\sin\Theta_i & \sin\Phi_i\cos\Theta_i & \cos\Phi_i\cos\Theta_i\end{bmatrix}\begin{bmatrix}u_i\\ v_i\\ w_i\end{bmatrix}, \quad (1)$$

$$\begin{bmatrix}\dot{\Phi}_i\\ \dot{\Theta}_i\\ \dot{\Psi}_i\end{bmatrix} = \begin{bmatrix}1 & \sin\Phi_i\tan\Theta_i & \cos\Phi_i\tan\Theta_i\\ 0 & \cos\Phi_i & -\sin\Phi_i\\ 0 & \sin\Phi_i\sec\Theta_i & \cos\Phi_i\sec\Theta_i\end{bmatrix}\begin{bmatrix}q_i\\ r_i\\ s_i\end{bmatrix}, \quad (2)$$

where $p_i = [x_i \;\; y_i \;\; z_i]^T$ is the position vector and $\Omega_i = [\Phi_i \;\; \Theta_i \;\; \Psi_i]^T$ is the vector of 3-2-1 Euler angles taken with respect to a global Cartesian coordinate frame $\mathcal{G}$ with origin $\mathcal{O}$. The linear velocities $[u_i \;\; v_i \;\; w_i]^T$ and angular velocities $[q_i \;\; r_i \;\; s_i]^T$ are both presented in the body fixed frame $\mathcal{B}_i$ with origin $p_i$. The state vector of agent $i$ is defined as $q_i = [p_i^T \;\; \Omega_i^T]^T$. In the sequel, the rotation matrices of (1) and (2) shall be denoted $\mathcal{R}_1$ and $\mathcal{R}_2$ respectively. The agents travel within a stationary domain, $\mathcal{D} \subset \mathbb{R}^3$. Their task is to survey a two-dimensional manifold, $\mathcal{C} \subset \mathcal{D}$, known as our surface of interest.

Each agent, $i$, is equipped with a forward facing sensor whose footprint shall be referred to as $\mathcal{S}_i$. A spherical sector model is chosen for $\mathcal{S}_i$ as it is representative of the space typically observable to a single camera lens. The authors also utilize this sensing model in [17] and [18]. $\mathcal{S}_i$ provides anisotropic sensing data which degrade in quality towards the periphery of the footprint in a similar manner to that of a camera lens. This is encoded through the definition of the sensing constraint functions for each agent $i$:

$$c_{1i} = R_i^2 - (\tilde{x} - x_i)^2 - (\tilde{y} - y_i)^2 - (\tilde{z} - z_i)^2, \quad (3a)$$

$$c_{2i} = \alpha_i - \phi_i, \quad (3b)$$

$$c_{3i} = \alpha_i + \phi_i, \quad (3c)$$

where $R_i$ is the sensing range, $\tilde{p}_i = [\tilde{x} \;\; \tilde{y} \;\; \tilde{z}]^T$ is the position of a point within $\mathcal{S}_i$ with respect to $\mathcal{G}$, $\alpha_i$ is the angle between the periphery and centerline of the spherical sector (the $\hat{x}_{\mathcal{B}_i}$ axis), and $\phi_i$ is the angle between $r_{\tilde{p}_i/p_i} = \tilde{p}_i - p_i$ (resolved in $\mathcal{G}$ by construction) and the $\hat{x}_{\mathcal{B}_i}$ axis. $\phi_i$ is the inverse cosine of the dot product of $\hat{r}_{\tilde{p}_i/p_i}$ and $\hat{x}_{\mathcal{B}_i}$ resolved in $\mathcal{G}$:

$$\phi_i = \arccos\left(\hat{r}_{\tilde{p}_i/p_i} \cdot \hat{x}_{\mathcal{B}_i}|_{\mathcal{G}}\right). \quad (4)$$

Note that:

$$\hat{r}_{\tilde{p}_i/p_i} = \frac{1}{\sqrt{(\tilde{x}-x_i)^2 + (\tilde{y}-y_i)^2 + (\tilde{z}-z_i)^2}}\begin{bmatrix}(\tilde{x}-x_i)\\ (\tilde{y}-y_i)\\ (\tilde{z}-z_i)\end{bmatrix},$$

and $\hat{x}_{\mathcal{B}_i}|_{\mathcal{G}}$ is determined by multiplying $\mathcal{R}_1$ by $[1 \;\; 0 \;\; 0]^T$:

$$\hat{x}_{\mathcal{B}_i}|_{\mathcal{G}} = \begin{bmatrix}\cos\Psi_i\cos\Theta_i\\ \sin\Psi_i\cos\Theta_i\\ -\sin\Theta_i\end{bmatrix}.$$

Agent $i$ is thus capable of detecting objects that lie within an angle of $2\alpha_i > 0$ about the $\hat{x}_{\mathcal{B}_i}$ axis and a range of $R_i > 0$. The model for agent $i$ is depicted in Fig. 1.

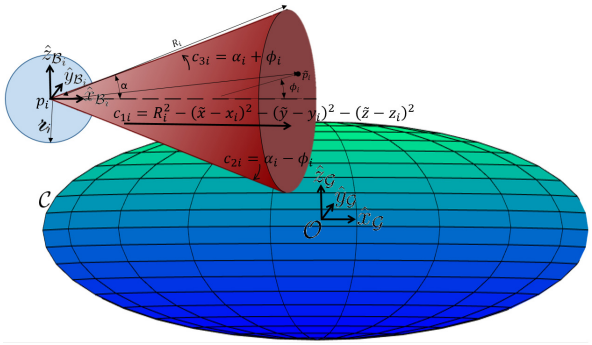


Fig. 1. Agent $i$ is modeled as a sphere of radius $r_i$ and has a forward facing sensor footprint, $\mathcal{S}_i$. Sensing constraint functions $c_{\ell i}$, $\forall \ell \in \{1,2,3\}$, encode a decay in sensing quality along the depth and towards the periphery of $\mathcal{S}_i$.

Let us define a barrier function in terms of the sensing constraint functions:

$$B_i = \frac{1}{\max\{0, c_{1i}\}} + \frac{1}{\max\{0, c_{2i}\}} + \frac{1}{\max\{0, c_{3i}\}}.$$

One can define the sensing function that represents the quality of information available at each point over the sensing domain as:

$$S_i(q_i, \tilde{p}) = \frac{1}{B_i}, \quad (5)$$

which takes a value of zero outside of $\mathcal{S}_i$. Define the coverage level provided by agent $i$ at time $t$ as:

$$Q_i(t, \tilde{p}) = \int_0^t S_i\left(q_i(\tau), \tilde{p}\right) C\left(\tilde{p}\right) d\tau, \quad (6)$$

where $C$ is defined as:

$$C\left(\tilde{p}\right) = \begin{cases}1, & \forall \tilde{p} \in \mathcal{C};\\ 0, & \forall \tilde{p} \notin \mathcal{C},\end{cases}$$

and encodes that the accumulation of sensing information only occurs along our surface of interest, $\mathcal{C}$.

As the agents cover $\mathcal{C}$, a set of $N_p$ high-speed particles denoted $k \in \{1, ..., N_p\}$, each of which travels at a constant linear velocity, pass through the domain. Each particle shall have an associated map decay term, $\Lambda_k\left(\tau, \tilde{p}\right)$, which is defined later in Section IV-B. We may now define the global coverage level:

$$Q(t, \tilde{p}) = \sum_{i=1}^{N} Q_i(t, \tilde{p}) - \sum_{k=1}^{N_p} \int_0^t \Lambda_k\left(\tau, \tilde{p}\right) C\left(\tilde{p}\right) d\tau. \quad (7)$$

*Definition 1:* Agent $i$ avoids collision so long as $\|p_i(t) - p_j(t)\| > r_i + r_j$, $\forall j \neq i \in \{1, ..., N\}$ and $\|n_i\| > r_i$ where the vector $n_i$ has direction normal to $\mathcal{C}$ and length equal to the Euclidean distance of its intersection point on $\mathcal{C}$ to $p_i$.

In this work, coverage refers to the accumulation of sensing data over time. Points, $\tilde{p}$, are said to be sufficiently covered when $Q\left(t, \tilde{p}\right) \geq C^\star$. The purpose of this work is to derive a control strategy which persistently sweeps $\mathcal{S}_i$ across $\mathcal{C}$ while emphasizing surveillance around the predicted impact points of particles $k \in \{1, ..., N_p\}$ on $\mathcal{C}$. This must be done while avoiding collisions as defined in *Definition 1*.

Expand $\frac{d}{dt}(S_i(q_i(t),\tilde{p}))$:

$$\begin{aligned}\frac{d}{dt}(S_i(q_i(t),\tilde{p})) &= \frac{\partial S_i}{\partial x_i}\dot{x}_i(t)+\frac{\partial S_i}{\partial y_i}\dot{y}_i(t)+\frac{\partial S_i}{\partial z_i}\dot{z}_i(t)+\frac{\partial S_i}{\partial \Psi_i}\dot{\Psi}_i(t)+\frac{\partial S_i}{\partial \Theta_i}\dot{\Theta}_i(t) = \left(\frac{\partial S_i}{\partial x_i}\cos\Theta\cos\Psi+\frac{\partial S_i}{\partial y_i}\cos\Theta\sin\Psi-\frac{\partial S_i}{\partial z_i}\sin\Theta\right)u_i(t)\\ &+\left(\frac{\partial S_i}{\partial x_i}(\sin\Phi\sin\Theta\cos\Psi-\cos\Phi\sin\Psi)+\frac{\partial S_i}{\partial y_i}(\sin\Phi\sin\Theta\sin\Psi+\cos\Phi\cos\Psi)+\frac{\partial S_i}{\partial z_i}\sin\Phi\cos\Theta\right)v_i(t)\\ &+\left(\frac{\partial S_i}{\partial x_i}(\cos\Phi\sin\Theta\cos\Psi+\sin\Phi\sin\Psi)+\frac{\partial S_i}{\partial y_i}(\cos\Phi\sin\Theta\sin\Psi-\sin\Phi\cos\Psi)+\frac{\partial S_i}{\partial z_i}\cos\Phi\cos\Theta\right)w_i(t)\\ &+\left(\frac{\partial S_i}{\partial \Psi_i}\sin\Phi\sec\Theta+\frac{\partial S_i}{\partial \Theta_i}\cos\Phi\right)r_i(t)+\left(\frac{\partial S_i}{\partial \Psi_i}\cos\Phi\sec\Theta-\frac{\partial S_i}{\partial \Theta_i}\sin\Phi\right)s_i(t).\end{aligned} \tag{14}$$

Now introduce the following definitions:

$$a_{i0}(t,Q(t,\tilde{p})) = \int_{D_i} h''(C^\star C(\tilde{p})-Q(t,\tilde{p}))S_i(q_i(t),\tilde{p})^2 C(\tilde{p})^2\,d\tilde{p}, \tag{15}$$

$$a_{i1}(t,Q(t,\tilde{p})) = \int_{D_i} h'(C^\star C(\tilde{p})-Q(t,\tilde{p}))C(\tilde{p})\left(\frac{\partial S_i}{\partial x_i}\cos\Theta\cos\Psi+\frac{\partial S_i}{\partial y_i}\cos\Theta\sin\Psi-\frac{\partial S_i}{\partial z_i}\sin\Theta\right)d\tilde{p}, \tag{16}$$

$$a_{i2}(t,Q(t,\tilde{p})) = \int_{D_i} h'(C^\star C(\tilde{p})-Q(t,\tilde{p}))C(\tilde{p})\left(\frac{\partial S_i}{\partial x_i}(\sin\Phi\sin\Theta\cos\Psi-\cos\Phi\sin\Psi)+\frac{\partial S_i}{\partial y_i}(\sin\Phi\sin\Theta\sin\Psi+\cos\Phi\cos\Psi)+\frac{\partial S_i}{\partial z_i}\sin\Phi\cos\Theta\right)d\tilde{p}, \tag{17}$$

$$a_{i3}(t,Q(t,\tilde{p})) = \int_{D_i} h'(C^\star C(\tilde{p})-Q(t,\tilde{p}))C(\tilde{p})\left(\frac{\partial S_i}{\partial x_i}(\cos\Phi\sin\Theta\cos\Psi+\sin\Phi\sin\Psi)+\frac{\partial S_i}{\partial y_i}(\cos\Phi\sin\Theta\sin\Psi-\sin\Phi\cos\Psi)+\frac{\partial S_i}{\partial z_i}\cos\Phi\cos\Theta\right)d\tilde{p}, \tag{18}$$

$$a_{i4}(t,Q(t,\tilde{p})) = \int_{D_i} h'(C^\star C(\tilde{p})-Q(t,\tilde{p}))C(\tilde{p})\left(\frac{\partial S_i}{\partial \Psi_i}\sin\Phi\sec\Theta+\frac{\partial S_i}{\partial \Theta_i}\cos\Phi\right)d\tilde{p}, \tag{19}$$

$$a_{i5}(t,Q(t,\tilde{p})) = \int_{D_i} h'(C^\star C(\tilde{p})-Q(t,\tilde{p}))C(\tilde{p})\left(\frac{\partial S_i}{\partial \Psi_i}\cos\Phi\sec\Theta-\frac{\partial S_i}{\partial \Theta_i}\sin\Phi\right)d\tilde{p}. \tag{20}$$

One can then rewrite (13) as:

$$\dot{\tilde{e}}_i(t) = a_{i0}(t,Q(t,\tilde{p}))-u_i(t)a_{i1}(t,Q(t,\tilde{p}))-v_i(t)a_{i2}(t,Q(t,\tilde{p}))-w_i(t)a_{i3}(t,Q(t,\tilde{p}))-r_i(t)a_{i4}(t,Q(t,\tilde{p}))-s_i(t)a_{i5}(t,Q(t,\tilde{p})). \tag{21}$$

---

## III. Persistent Coverage Control

Define the global coverage error with respect to $C^\star$ as:

$$E(t) = \int_{\mathcal{D}} h\left(C^\star C(\tilde{p})-Q(t,\tilde{p})\right)d\tilde{p}, \tag{8}$$

where $h(w) = (\max\{0,w\})^3$ with first derivative $h' = \frac{dh}{dw} = 3(\max\{0,w\})^2$ and second derivative $h'' = \frac{d^2h}{dw^2} = 6(\max\{0,w\})$. Our persistent coverage control laws will be derived via differentiation of (8), a volume integral, so a few mathematical preliminaries are required.

Recall the generalized transport theorem [20]:

$$\frac{d}{dt}\int_{R_{(s)}} f\,dV = \int_{R_{(s)}}\frac{\partial f}{\partial t}\,dV+\int_{S_{(s)}} f\mathbf{v}_{(\mathbf{s})}\cdot\mathbf{n}\,dA \tag{9}$$

where $f$ is any scalar-, vector-, or tensor-valued function of position and time, $S_{(s)}$ is the boundary of the volume $R_{(s)}$ over which $f$ is integrated, $\mathbf{n}$ is the unit vector normal to the boundary, and $\mathbf{v}_{(\mathbf{s})}$ is the velocity of the boundary. $V$ and $A$ refer to volume and area respectively. Invoking (9) allows for differentiation of (8) with respect to time:

$$\begin{aligned}\dot{E}(t) = &\int_{\mathcal{D}} h'(C^\star C(\tilde{p})-Q(t,\tilde{p}))\left(\frac{-\partial Q(t,\tilde{p})}{\partial t}\right)d\tilde{p}\\ &+\int_{\partial\mathcal{D}}\big(h(C^\star C(\tilde{p})-Q(t,\tilde{p}))\big)\mathbf{v}_{(\mathbf{s})}\cdot\mathbf{n}\,dA,\end{aligned} \tag{10}$$

where $\partial\mathcal{D}$ is the boundary of $\mathcal{D}$. The control volume is $\mathcal{D}$ which is time invariant and thus $\mathbf{v}_{(\mathbf{s})} = 0$. This expression reduces to:

$$\dot{E}(t) = \int_{D} h'(C^\star C(\tilde{p})-Q(t,\tilde{p}))\left(\frac{-\partial Q(t,\tilde{p})}{\partial t}\right)d\tilde{p}, \tag{11}$$

which expands to:

$$\begin{aligned}\dot{E}(t) &= -\int_D h'(C^\star C(\tilde{p})-Q(t,\tilde{p}))\Big(\sum_{i=1}^{N} S_i(q_i(t),\tilde{p})C(\tilde{p})\\ &\quad-\sum_{k=1}^{N_p}\Lambda_k(t,\tilde{p})C(\tilde{p})\Big)d\tilde{p}\\ &= \sum_{i=1}^{N}\underbrace{\int_D -h'(C^\star C(\tilde{p})-Q(t,\tilde{p}))S_i(q_i(t),\tilde{p})C(\tilde{p})\,d\tilde{p}}_{=\hat{e}_i(t)}\\ &\quad-\sum_{k=1}^{N_p}\underbrace{\int_D -h'(C^\star C(\tilde{p})-Q(t,\tilde{p}))\Lambda_k(t,\tilde{p})C(\tilde{p})\,d\tilde{p}}_{=\tilde{e}_k(t)}\\ &= \sum_{i=1}^{N}\hat{e}_i(t)-\sum_{k=1}^{N_p}\tilde{e}_k(t).\end{aligned} \tag{12}$$

$\hat{e}_i(t)$ is the rate of change of the coverage error due to the motion of the agents while $\tilde{e}_k(t)$ is the rate of change of the coverage error due to a contrived information decay surrounding the predicted impact point of particle $k$ on $\mathcal{C}$.

Our strategy is to control the agents' kinematics, recovered in the derivative of $\hat{e}_i(t)$, to decrease (12). Using this strategy, the agents actively seek to increase their rate of coverage by rotating and/or translating $\mathcal{S}_i$ to be encompass the most uncovered space in the local vicinity.

Taking the derivative of $\hat{e}_i(t)$ with respect to time yields:

$$\dot{\hat{e}}_i(t) = \int_{D_i} \Big( h''(C^\star C(\tilde{p}) - Q(t,\tilde{p}))S_i(q_i(t),\tilde{p})^2 C(\tilde{p})^2 - h'(C^\star C(\tilde{p}) - Q(t,\tilde{p}))\frac{d}{dt}(S_i(q_i(t),\tilde{p}))C(\tilde{p}) \Big) d\tilde{p}. \quad (13)$$

The sensing footprint is independent of $\Phi_i$ assuming that the centerline of the spherical sector is aligned with the $\hat{x}_{\mathcal{B}_i}$ axis. $\frac{d}{dt}(S_i(q_i(t),\tilde{p}))$ is expanded in (14) and through the definitions in (15-20) one may restate (13) as (21). If one were to command zero inputs to this system, it becomes clear that $a_{i0}(t, Q(t,\tilde{p}))$ may be physically interpreted as the rate at which the coverage rate is reducing due to information saturation at any particular position and orientation of the sensing footprint, $\mathcal{S}_i$. As the footprint remains stationary, there are diminishing returns on the value of newly acquired information. Thus, the additional terms in (21) allow for the coverage rate to be increased by mobilizing the sensor. One strategy is to define the following control law:

$$u_i = k_u \frac{a_{i1}(t,\acute{Q}_i(t,\tilde{p}))}{\sqrt{a_{i1}^2 + a_{i2}^2 + a_{i3}^2}} + \hat{x}_{\mathcal{B}_i} \cdot \rho_{l,i}, \quad (22a)$$

$$v_i = k_v \frac{a_{i2}(t,\acute{Q}_i(t,\tilde{p}))}{\sqrt{a_{i1}^2 + a_{i2}^2 + a_{i3}^2}} + \hat{y}_{\mathcal{B}_i} \cdot \rho_{l,i}, \quad (22b)$$

$$w_i = k_w \frac{a_{i3}(t,\acute{Q}_i(t,\tilde{p}))}{\sqrt{a_{i1}^2 + a_{i2}^2 + a_{i3}^2}} + \hat{z}_{\mathcal{B}_i} \cdot \rho_{l,i}, \quad (22c)$$

$$r_i = \bar{r}_i sat\Big(\frac{k_r a_{i4}(t,\acute{Q}_i(t,\tilde{p}))}{\bar{r}_i}\Big) + \hat{y}_{\mathcal{B}_i} \cdot \rho_{a,i}, \quad (22d)$$

$$s_i = \bar{s}_i sat\Big(\frac{k_s a_{i5}(t,\acute{Q}_i(t,\tilde{p}))}{\bar{s}_i}\Big) + \hat{z}_{\mathcal{B}_i} \cdot \rho_{a,i}, \quad (22e)$$

where:

$$\rho_{l,i} = -\ln\left(\frac{1}{\gamma R_i - \not{z}_i}(\|n_i\| - r_i)\right)\mathcal{R}_1^{-1}\hat{n}_i, \quad (23)$$

$$\rho_{a,i} = \xi\mathcal{R}_2^{-1}\begin{bmatrix} 0 \\ \arcsin(\hat{n}_i \cdot \hat{z}_\mathcal{G}) - \Theta_i \\ \text{atan2}(-\hat{n}_i \cdot \hat{y}_\mathcal{G}, -\hat{n}_i \cdot \hat{x}_\mathcal{G}) - \Psi_i \end{bmatrix}, \quad (24)$$

and $\hat{n}_i$ is a unit vector parallel to $n_i$. Note that the denominator terms in (22 a-c) share the same functional dependencies as the numerator which are omitted in the interest of space. $\rho_{l,i}$ is a collision avoidance term with respect to the surface of interest. It takes a value of zero when agent $i$'s normalized distance from $\mathcal{C}$ is $\gamma R_i$ for $\gamma \in (0,1]$ and is logarithmically repulsive and attractive from the surface when the distance is decreased or increased respectively. $\rho_{a,i}$, for $\xi << 1$, encodes that the agents should tend to align $\hat{x}_{\mathcal{B}_i}$ with $-\hat{n}_i$ if the coverage terms associated with $r_i$ and $s_i$ have become sufficiently small. The physical meaning of $\rho_{a,i}$ is to direct $\mathcal{S}_i$ back onto $\mathcal{C}$ if it has reached a configuration in which it no longer intersects $\mathcal{C}$. See Fig. 2 for further illustration of the effects of $\rho_{l,i}$ and $\rho_{a,i}$.

The left-hand additive terms in (22) are designed to reduce (21) by matching the sign and relative magnitudes of

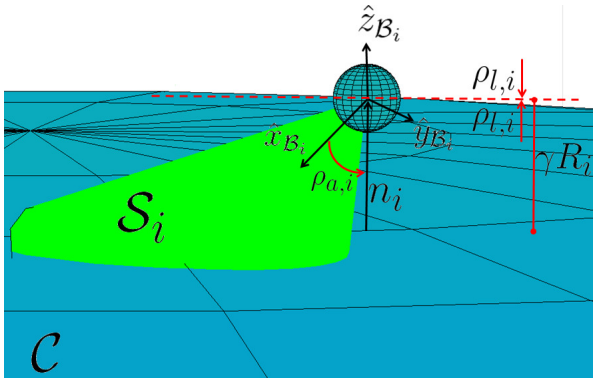


Fig. 2. As agent $i$ explores $\mathcal{C}$, $\rho_{l,i}$ is parallel to $n_i$ for $\|n_i\| < \gamma R_i$, antiparallel to $n_i$ for $\|n_i\| > \gamma R_i$, and the zero vector otherwise. This term prevents collision of $i$ with $\mathcal{C}$ and prevents $i$ from flying away from $\mathcal{C}$. $\rho_{a,i}$ tends to direct $\mathcal{S}_i$ onto $\mathcal{C}$.

$a_{i,\ell}$, $\forall \ell \in \{1,....,5\}$. $\bar{r}_i$ and $\bar{s}_i$ are saturation limits for the coverage angular velocity inputs to the system. Note that the agents actual commanded velocities are unbounded as initial conditions may be chosen with agents arbitrarily close to the surface $\mathcal{C}$.

The coverage control laws are functions of $\acute{Q}_i(t,\tilde{p})$, a modified coverage map of agent $i$, which may be defined in terms of:

$$\acute{Q}_{ij}(t,\tilde{p}) = \begin{cases} M_{1i}(p_j,\tilde{p}), & \text{if } \|p_i - p_j\| \le R_i; \\ 0, & \text{otherwise,} \end{cases} \quad (25)$$

where:

$$M_{1i}(p_j,\tilde{p}) = \begin{cases} C^\star, & \text{if } \tilde{p} \in \bar{B}_{R_{b,ij}}(p_j); \\ 0, & \text{otherwise,} \end{cases} \quad (26)$$

and $\bar{B}_{R_{b,ij}}(p_j)$ is the closed ball of radius $R_{b,ij}$ centered at $p_j$. $\acute{Q}_{ij}(t,\tilde{p})$ augments the global coverage map for $i$ as follows: $\acute{Q}_i(t,\tilde{p}) = Q(t,\tilde{p}) + \sum_{j=1}^{N-1}\acute{Q}_{ij}(t,\tilde{p})$. Essentially, portions of the map are defined with a coverage value of $C^\star$ around each agent $j \neq i \in \{1,...,N\}$. These are added to $Q(t,\tilde{p})$ to encode inter-agent collision avoidance in (22). This strategy is fully described in our previous work [21] and rigorously proven to guarantee collision avoidance.

## IV. Information Decay

### A. Particle Measurement and State Estimation

We assume that an omnidirectional range sensor (e.g., LiDAR) is co-located with $\mathcal{O}$ and provides measurements of each particle's position in spherical coordinates. Define a model for the motion of particle $k$:

$$\dot{\tilde{q}}_k(t) = \begin{bmatrix} 0_{3\times3} & \mathbb{I}_{3\times3} \\ 0_{3\times3} & 0_{3\times3} \end{bmatrix}\tilde{q}_k(t), \quad (27)$$

$$\tilde{z}_k(t) = \begin{bmatrix} \sqrt{x_k^2 + y_k^2 + z_k^2} \\ \text{atan2}(y_k, x_k) \\ \arccos\left(\frac{z_k}{\sqrt{x_k^2+y_k^2+z_k^2}}\right) \end{bmatrix} + \epsilon, \quad (28)$$

where $\tilde{q}_k = [x_k, y_k, z_k, \dot{x}_k, \dot{y}_k, \dot{z}_k]^T$ and $\tilde{z}_k = [\rho_k, \theta_k, \psi_k]^T$ are the Cartesian state and spherical coordinate

measurement vectors of particle $k$ resolved in $\mathcal{G}$. $\rho_k$, $\theta_k$, and $\psi_k$ are the range, azimuthal angle, and polar angle of $k$ respectively. In the sequel, the matrix in (28) shall be denoted $\tilde{h}(x_k, y_k, z_k)$. Assume that the measurement noise, $\epsilon$, is zero-mean Gaussian and has covariance $\mathbf{R} = diag\left(\sigma_\rho^2, \sigma_\theta^2, \sigma_\psi^2\right)$. This system models high-speed particles incident upon a surface with negligible drag (e.g., micrometeoroids impacting a spacecraft hull); thus, it is reasonable to omit the process noise. The state and covariance estimates, $\hat{\tilde{q}}$ and $\mathbf{P}_k$, are computed with a continuous-time extended Kalman filter:

$$\dot{\hat{\tilde{q}}}_k(t) = \begin{bmatrix} 0_{3\times3} & \mathbb{I}_{3\times3} \\ 0_{3\times3} & 0_{3\times3} \end{bmatrix} \tilde{q}_k(t) + \mathbf{K}\left(\tilde{z}_k(t) - \tilde{h}(\hat{x}_k, \hat{y}_k, \hat{z}_k)\right), \tag{29}$$

$$\dot{\mathbf{P}}_k(t) = \mathbf{F}\mathbf{P}_k(t) + \mathbf{P}_k(t)\mathbf{F}^T - \mathbf{K}(t)\mathbf{H}(t)\mathbf{P}_k(t), \tag{30}$$

with Kalman gain $\mathbf{K}(t) = \mathbf{P}_k(t)\mathbf{H}(t)\mathbf{R}^{-1}$ and:

$$\mathbf{F} = \begin{bmatrix} 0_{3\times3} & \mathbb{I}_{3\times3} \\ 0_{3\times3} & 0_{3\times3} \end{bmatrix},$$

$$\mathbf{H}(t) = \begin{bmatrix} \frac{\hat{x}_k}{\sqrt{\hat{x}_k^2+\hat{y}_k^2+\hat{z}_k^2}} & \frac{\hat{y}_k}{\sqrt{\hat{x}_k^2+\hat{y}_k^2+\hat{z}_k^2}} & \frac{\hat{z}_k}{\sqrt{\hat{x}_k^2+\hat{y}_k^2+\hat{z}_k^2}} & 0_{1\times3} \\ \frac{-\hat{y}_k}{\hat{x}_k^2+\hat{y}_k^2} & \frac{\hat{x}_k}{\hat{x}_k^2+\hat{y}_k^2} & 0 & 0_{1\times3} \\ \frac{\hat{x}_k\hat{z}_k\left(1-\frac{\hat{z}_k^2}{\hat{x}_k^2+\hat{y}_k^2+\hat{z}_k^2}\right)^{-1/2}}{\left(\hat{x}_k^2+\hat{y}_k^2+\hat{z}_k^2\right)^{3/2}} & \frac{\hat{y}_k\hat{z}_k\left(1-\frac{\hat{z}_k^2}{\hat{x}_k^2+\hat{y}_k^2+\hat{z}_k^2}\right)^{-1/2}}{\left(\hat{x}_k^2+\hat{y}_k^2+\hat{z}_k^2\right)^{3/2}} & -\frac{\frac{1}{\sqrt{\hat{x}_k^2+\hat{y}_k^2+\hat{z}_k^2}}-\frac{\hat{z}_k^2}{\left(\hat{x}_k^2+\hat{y}_k^2+\hat{z}_k^2\right)^{3/2}}}{\sqrt{1-\frac{\hat{z}_k^2}{\hat{x}_k^2+\hat{y}_k^2+\hat{z}_k^2}}} & 0_{1\times3} \end{bmatrix}.$$

If particle $k$ is detected at time $t_{dk}$, we initialize the state estimate at $t_{dk'} = t_{dk} + \Delta t$ using measurements $\tilde{z}_k(t_{dk})$ and $\tilde{z}_k(t_{dk'})$ as follows:

$$\hat{\tilde{q}}_k(t_{dk'}) = \begin{bmatrix} \rho_k(t_{dk'})\cos\theta_k(t_{dk'})\sin\psi_k(t_{dk'}) \\ \rho_k(t_{dk'})\sin\theta_k(t_{dk'})\sin\psi_k(t_{dk'}) \\ \rho_k(t_{dk'})\cos\psi_k(t_{dk'}) \\ \frac{\rho_k(t_{dk'})\cos\theta_k(t_{dk'})\sin\psi_k(t_{dk'})-\rho_k(t_{dk})\cos\theta_k(t_{dk})\sin\psi_k(t_{dk})}{\Delta t} \\ \frac{\rho_k(t_{dk'})\sin\theta_k(t_{dk'})\sin\psi_k(t_{dk'})-\rho_k(t_{dk})\sin\theta_k(t_{dk})\sin\psi_k(t_{dk})}{\Delta t} \\ \frac{\rho_k(t_{dk'})\cos\psi_k(t_{dk'})-\rho_k(t_{dk})\cos\psi_k(t_{dk})}{\Delta t} \end{bmatrix},$$

where $\Delta t$ is lower bounded by the time required to record two measurements of $\tilde{z}_k(t)$. Thus $\Delta t$ may be arbitrarily small in continuous time. Although estimate errors are correlated, it is reasonable to select a diagonal matrix for the the initialization $\mathbf{P}_k(t_{dk'})$. We define these diagonal elements of $\mathbf{P}_k(t_{dk'})$ using the propagation of errors formula presented as equation (3.47) in [22]. Thus, element $(\ell,\ell)$, $\forall \ell \in \{1,...,6\}$, of $\mathbf{P}_k(t_{dk'})$ is defined as the sum of squares of each measurement uncertainty multiplied by the partial derivative of element $\ell$ of $\hat{\tilde{q}}_k(t_{dk'})$ with respect to that associated measurement variable. The analytic form of $\mathbf{P}_k(t_{dk'})$ is omitted in the interest of space.

### B. Decay Rate Map Evolution

At any time $t$, we define our decay rate map for particle $k$ in terms of its predicted position and covariance evolution over a horizon $T_{H,k}(t)$. As the particles are assumed to travel at fixed velocities, the predicted values for Cartesian position $\tilde{p}'_k(t+\tau)$ and associated covariance $\mathbf{P}_k(t+\tau)$ may be defined as $\tilde{p}'_k(t+\tau) = F\hat{\tilde{q}}_k(t)$, and $\mathbf{P'}_k(t+\tau) = F\mathbf{P}_k(t)F^T$, where:

$$F = \begin{bmatrix} 1 & 0 & 0 & \tau & 0 & 0 \\ 0 & 1 & 0 & 0 & \tau & 0 \\ 0 & 0 & 1 & 0 & 0 & \tau \end{bmatrix}.$$

We define the decay rate map associated with particle $k$ as the integral of our predicted normal distribution $\mathcal{N}(\tilde{p}'_k(t+\tau), \mathbf{P'}_k(t+\tau))$ through horizon $T_H$:

$$\Lambda_k(t,\tilde{p}) = \int_0^{T_{H,k}(t)} \lambda_k \mathcal{N}\left(\tilde{p}'_k(t+\tau), \beta\mathbf{P'}_k(t+\tau)\right) d\tau. \tag{31}$$

For $t < t_{dk'}$, define $\Lambda_k(t,\tilde{p}) = 0$, $\forall \tilde{p} \in \mathcal{D}$. Our formulation for (31) essentially takes a normal distribution for the position of particle $k$ at time $t$ and cumulatively sweeps it forward in time up to our horizon $T_{H,k}(t)$. The horizon is lower-bounded by an estimate of the remaining time until impact of particle $k$ on $\mathcal{C}$. This may be computed using $\tilde{q}_k(t)$ along with the surface geometry. With this design, $Q(t,\tilde{p})$ decays along the predicted trajectory of $k$ with tapering omnidirectional decay rates spreading out from the predicted path. This design lends itself naturally to our local coverage formulation, which is gradient following in nature, in that the agents may follow these tapered decay paths towards the predicted impact points on our surface of interest. The parameter $\lambda_k > 0$ may be adjusted to scale how rapidly the coverage level will decay in time. Furthermore, $\mathbf{P'}_k$ is scaled by a factor of $\beta > 0$ to widen the tails of the distribution such that they may cover the entire surface of interest $\mathcal{C}$. This is necessary to guarantee a sufficiently large coverage gradient exists over the entire surface in spite of high precision measurements. As a design guideline, one may choose the two furthest points on a surface and select a value for $\beta$ such that a particle impacting one point will result in a 3-sigma value for $\mathcal{N}\left(\tilde{p}'_k(t+\tau), \beta\mathbf{P'}_k(t+\tau)\right)$ at the other point.

## V. Simulations

A simulation was performed in MATLAB to verify the efficacy of the algorithm. Three agents, denoted $i \in \{1,2,3\}$, are deployed to cover the surface of an ellipsoid, $\mathcal{C}$, whose radius in the $xy$-plane is 80 and whose radius in the $z$-plane is 20. For each agent, $R_i = 10$, $\mathbb{z}_i = 1$, $\alpha_i = 30°$, $k_u = 1$, $k_v = 5$, $k_w = 1$, $k_r = 0.1$, $k_s = 0.1$, $\bar{r}_i = 0.4$, $\bar{s}_i = 0.4$. Upon initialization of the simulation, $\mathcal{C}$ was set to a fully covered level of $C^\star = 20$ which would begin decaying upon detection of the first particle $k \in \{1,...,4\}$ at $t = 1$ sec. Particles, which travelled in random directions at a speed of 40 distance units per second, were generated every 40 seconds. Position measurements of the particles had noise characterized by $\sigma_\rho = 0.5$, $\sigma_\theta = .09$, and $\sigma_\psi = 0.09$. For the decay-rate map, the parameters $\beta = 1$ and $\lambda_k = 0.1$ yielded desirable performance in simulation allowing agents to orient

themselves with respect to the gradient of the coverage error regardless of their distance from the predicted impact points. Time-lapse plots of the agents' trajectories in response to particle $k = 1$ are presented in Fig. 3. The normalized coverage level of the domain as well as inter-agent distances are presented in Fig. 4.

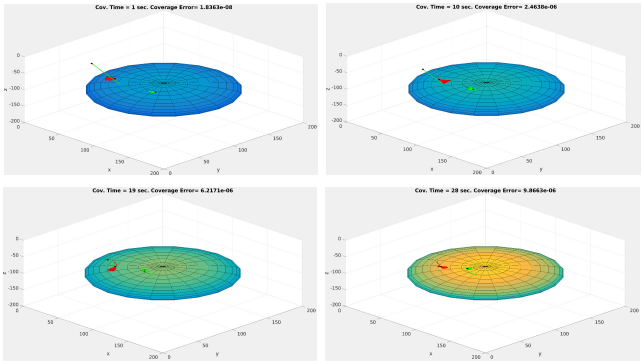


Fig. 3. Agent $i = 2$ and $i = 3$ track towards the impact point of particle $k = 1$. True and estimated trajectories of $k = 1$ are indicated in green and red. $i = 2$ and $i = 3$ trajectories are curved and indicated in red and green.

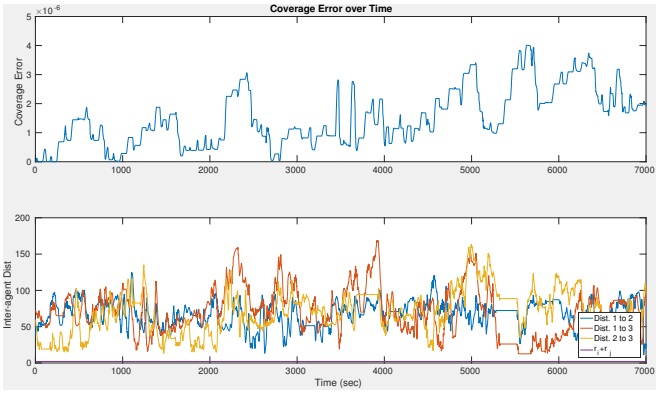


Fig. 4. Disturbances spike the coverage error up from zero while agents effectively maintain an error on the order of $10^{-6}$. Inter-agent distances are well above $r_i + r_j = 2$.

Over the course of 7000 seconds of simulation time, the agents were able to avoid collision and cover effectively at the impact points of particles. The coverage error tended to oscillate between $0.5 \times 10^{-6}$ and $4 \times 10^{-6}$.

## VI. Conclusions

In this paper, we presented a novel persistent coverage algorithm for agents sweeping spherical sector sensing footprints over a 2-D manifold. The manifold was continuously impacted by high-speed particles whose trajectories were estimated online using an extended Kalman filter. The predicted impact points on the manifold, along with their associated covariances, were used to design an information decay rate map which guided the motion of the agents in the time immediately preceding and following the impacts. The algorithm was verified in simulation

## References


[1] T. Bokareva, W. Hu, S. Kanhere, B. Ristic, N. Gordon, T. Bessell, M. Rutten, and S. Jha, "Wireless sensor networks for battlefield surveillance," in *Proceedings of the land warfare conference*, 2006, pp. 1–8.

[2] R. R. Murphy, S. Tadokoro, D. Nardi, A. Jacoff, P. Fiorini, H. Choset, and A. M. Erkmen, "Search and rescue robotics," in *Springer Handbook of Robotics*. Springer Berlin Heidelberg, 2008, pp. 1151–1173.

[3] H. Choset and D. Kortenkamp, "Path planning and control for free-flying inspection robot in space," *Journal of Aerospace Engineering*, vol. 12, no. 2, pp. 74–81, 1999.

[4] G. A. Hollinger, B. Englot, F. S. Hover, U. Mitra, and G. S. Sukhatme, "Active planning for underwater inspection and the benefit of adaptivity," *The International Journal of Robotics Research*, vol. 32, no. 1, pp. 3–18, 2013.

[5] J. Cortes, S. Martínez, T. Karatas, and F. Bullo, "Coverage control for mobile sensing networks," *IEEE Trans. on Robotics and Automation*, vol. 20, no. 2, pp. 243–255, 2004.

[6] A. Kwok and S. Martínez, "Energy-balancing cooperative strategies for sensor deployment," in *Proc. of the 2007 IEEE Conference on Decision and Control*, New Orleans, LA, Dec. 2007, pp. 6136–6141.

[7] A. Kwok and S. Martinez, "Deployment algorithms for a power-constrained mobile sensor network," in *Proc. of the 2008 IEEE International Conference on Robotics and Automation*, Pasadena, CA, may 2008, pp. 140–145.

[8] I. I. Hussein and D. M. Stipanović, "Effective coverage control for mobile sensor networks with guaranteed collision avoidance," *IEEE Trans. on Control Systems Technology*, vol. 15, no. 4, pp. 642–657, Jul. 2007.

[9] B. Liu, O. Dousse, P. Nain, and D. Towsley, "Dynamic coverage of mobile sensor networks," *IEEE Transactions on Parallel and Distributed systems*, vol. 24, no. 2, pp. 301–311, 2013.

[10] D. M. Stipanović, C. Valicka, C. J. Tomlin, and T. R. Bewley, "Safe and reliable coverage control," *Numerical Algebra, Control and Optimization*, vol. 3, pp. 31–48, 2013.

[11] P. Hokayem, D. Stipanovíc, and M. Spong, "On persistent coverage control," in *Proc. of the 2007 IEEE Conference on Decision and Control*, New Orleans, LA, USA, Dec. 2007, pp. 6130–6135.

[12] C. Song, L. Liu, G. Feng, Y. Wang, and Q. Gao, "Persistent awareness coverage control for mobile sensor networks," *Automatica*, vol. 49, no. 6, pp. 1867–1873, 2013.

[13] S. L. Smith, M. Schwager, and D. Rus, "Persistent robotic tasks: Monitoring and sweeping in changing environments," *IEEE Transactions on Robotics*, vol. 28, no. 2, pp. 410–426, 2012.

[14] N. Hübel, S. Hirche, A. Gusrialdi, T. Hatanaka, M. Fujita, and O. Sawodny, "Coverage control with information decay in dynamic environments," in *Proc. of the 17th IFAC World Congress*, Seoul, South Korea, Jul. 2008, pp. 4180–4185.

[15] C. Song, G. Feng, Y. Fan, and Y. Wang, "Decentralized adaptive awareness coverage control for multi-agent networks," *Automatica*, vol. 47, no. 12, pp. 2749 – 2756, 2011. [Online]. Available: http://www.sciencedirect.com/science/article/pii/S0005109811004328

[16] P. Cheng, J. Keller, and V. Kumar, "Time-optimal UAV trajectory planning for 3D urban structure coverage," in *Proc. of the 2008 IEEE/RSJ International Conference on Intelligent Robots and Systems*, Nice, France, Sep. 2008, pp. 2750–2757.

[17] W. Bentz and D. Panagou, "3D dynamic coverage and avoidance control in power-constrained uav surveillance networks," in *Submitted to the 2017 International Conference on Unmanned Aircraft Systems, under review*, Miami, FL, Jun. 2017.

[18] W. Bentz, T. Hoang, E. Bayasgalan, and D. Panagou, "Complete 3-D dynamic coverage in energy-constrained multi-uav sensor networks," *Submitted to Autonomous Robots, under review*.

[19] R. W. Beard, "Quadrotor dynamics and control," 2008, lecture notes.

[20] J. C. Slattery, *Advanced Transport Phenomena*. Cambridge UP, 1999.

[21] W. Bentz and D. Panagou, "An energy-aware redistribution method for multi-agent dynamic coverage networks," in *Proc. of the 2016 IEEE Conference on Decision and Control*, Las Vegas, NV, Dec. 2016.

[22] J. Taylor, *An Introduction to Error Analysis: The Study of Uncertainties in Physical Measurements*, ser. A series of books in physics. University Science Books, 1997. [Online]. Available: https://books.google.com/books?id=giFQcZub80oC